Applied Chemistry Project

Project title	Synthesis of Titania-Silica-Iron Oxide Nanocomposites and Investigation of their Bactericidal Activities

Student names	Miss Penpatcha Limsowan	ID	6033829123
	Miss Chutima Rakyu	ID	6033850223
Program	Bachelor of Science in Applied Chemistry		
Academic year	2020		

Faculty of Science, Chulalongkorn University

Synthesis of Titania-Silica-Iron Oxide Nanocomposites and Investigation of their Bactericidal Activities

by

Miss Penpatcha Limsowan

Miss Chutima Rakyu

In Partial Fulfillment for the Degree of Bachelor of Science

Program in Applied Chemistry (International Program)

Department of Chemistry, Faculty of Science

Chulalongkorn University

Academic Year 2020

Project   Synthesis of Titania-Silica-Iron Oxide Nanocomposites and Investigation of Their
            Bactericidal Activities

By   Miss Penpatcha Limsowan and Miss Chutima Rakyu

Accepted by Department of Chemistry, Faculty of Science, Chulalongkorn University in Partial Fulfillment of the Requirements for the Degree of Bachelor of Science Program in Applied Chemistry (International Program)

Examination committees
1. Assistant Professor Nipaka Sukpirom, PhD.   Chairman
2. Assistant Professor Pannee Leeladee, PhD.   Committee
3. Assistant Professor Numpon Insin, PhD.   Advisor

Endorsed and approved by the Head of Department of Chemistry

....
(Assistant Professor Numpon Insin, PhD.)   (Associate Professor Voravee Hoven, PhD.)
            Advisor   Head of Department of Chemistry

                                            Date ..28.. December 2020

Project Title: Synthesis of Titania-Silica-Iron Oxide Nanocomposites and Investigation of Their Bactericidal Activities

Student Name: Miss Penpatcha Limsowan   Student ID 6033829123

Miss Chutima Rakyu   Student ID 6033850223

Advisor Name: Assistant Professor Dr. Numpon Insin

Department of Chemistry, Faculty of Science, Chulalongkorn University, Academic Year 2020

Abstract

The multipurpose nanocomposites that combine superparamagnetic character, high photocatalytic activity with ability to degrade dye (methylene blue) and kill bacteria were synthesized and investigated. The magnetic nanocomposites consist of magnetite (Fe_3O_4) as the inner core, silica (SiO_2) as a middle layer and titania (TiO_2) as the outer shell. In order to synthesize the Titania-Silica-Iron Oxide Nanocomposites, a co-precipitation method was required to be used for both synthesis of iron oxide and coating silica layer. Besides, synthesis of titania shell was conducted by both co-precipitation and reverse microemulsion method. X-ray diffraction (XRD), scanning electron microscopy (SEM) and transmission electron microscopy (TEM) were used to characterize the prepared materials. Moreover, the photocatalytic activity of the synthesized nanocomposites was analyzed by using UV-visible absorption spectroscopy. According to the experiment, the thickness of the silica layer had been varied by differing the amount of TEOS at the ratio of 37.5, 150, 300, 600 and 900μL/ 0.1 g magnetite. The result demonstrates that the nanocomposites consisting of 600 μL TEOS exhibits the highest efficiency of degrading the methylene blue. However, the nanocomposites revealed the inefficiency for bactericidal properties under the irradiation of blue UV blacklight. The products from the synthesis by using co-precipitation method were collected in larger amounts when compared with previous work [1] and could lead to the large-scale production of materials for wastewater treatment applications.

Keywords: Nanocomposite, Bactericidal Activity, Photocatalyst, Titania, Magnetic

Acknowledgement

Firstly, I would really like to thank the BSAC program, the Department of Chemistry, Faculty of Science, Chulalongkorn University, for providing us a golden opportunity to do this project that we have never learned and done wherever before. This made us come to know many new things that we really need to apply in our real life in the future.

Foremost, we would like to express my deep and sincere gratitude to our project advisor, Assistant Professor Dr. Numpon Insin who always gives us all support and guidance for all the time during working on our senior project. For all his motivation, kindness, colossal knowledge and eagerness, we could not imagine how our project could be successful without a kindly assistance from our project advisor.

In addition, besides our advisor, we would like to thank our committee, Assistant Professor Dr. Pannee Leeladee, for activating and devoting her time to support and guidance us with a lot of insightful comments and useful questions.

Moreover, my sincere thanks also goes to Miss Padtaraporn Chanhom, Mr. Chonnavee Manipuntee and all staff members who are the senior members in our advisor project's laboratory, for giving us with fond greetings, supporting, teaching and encouraging, all the things that we could not find and this moment would hold in our memory forever.

Lastly, we are extremely grateful to our parents who always encourage and provide us with everything that we could not find any words to express this feeling, but we know unconditional support from them. So, without them we definitely could not finish this project for sure.

Penpatcha Limsowan

Chutima Rakyu

Table of Contents

Page

LIST OF TABLES   **Pages**

LIST OF FIGURES

LIST OF ABBREVIATIONS

TEOS	Tetraethyl orthosilicate
TBOT	Tetrabutyl orthotitanate
STEC	Shiga toxin-producing Escherichia coli
E. coli	*Escherichia coli*
$Fe_3O_4@SiO_2@TiO_2$	Magnetite/Iron Oxide (core)- Silica (interlayer)-Titania (shell) nanocomposite
1250TS150F_HexOH or Sample A	1250 μL of Titania (TBOT) - 150 μL of silica (TEOS) - 0.1 g of magnetite/ Iron oxide in hexanol solvent
125TS150F_EtOH or Sample B	125 μL of Titania (TBOT) - 150 μL of silica (TEOS) - 0.1 g of magnetite/ Iron oxide in ethanol solvent
375TS1505F_EtOH or Sample C	375 μL of Titania (TBOT) - 150 μL of silica (TEOS) - 0.1 g of magnetite/ Iron oxide in ethanol solvent
1250TS37.5F_EtOH or Sample D	1250 μL of Titania (TBOT) - 37.5 μL of silica (TEOS) - 0.1 g of magnetite/ Iron oxide in ethanol solvent
1250TS150F_EtOH or Sample E	1250 μL of Titania (TBOT) - 150 μL of silica (TEOS) - 0.1 g of magnetite/ Iron oxide in ethanol solvent
1250TS600F_EtOH or Sample F	1250 μL of Titania (TBOT) - 600 μL of silica (TEOS) - 0.1 g of magnetite/ Iron oxide in ethanol solvent
1250TS900F_EtOH or Sample G	1250 μL of Titania (TBOT) - 900 μL of silica (TEOS) - 0.1 g of magnetite/ Iron oxide in ethanol solvent
1250Titania_EtOH or Sample H	1250 μL of Titania (TBOT) in ethanol solvent
NPs	Nanoparticles
XRD	X-ray diffraction
TEM	Transmission Electron Microscope/Microscopy
SEM	Scanning Electron Microscope/Microscopy
EDX	Energy-dispersive X-ray
UVA	Ultraviolet A-rays
CTAB	Cetyl Trimethyl Ammonium Bromide
RPM	Revolutions per minute
pH	Potential of hydrogen
μL	Microliter
°C	Celsius
g	Gram

mg	Milligram
mL	Milliliter
min	Minute
h	Hour
kV	Kilovolt
mA	Milliampere
W	Watt
ppm	Part Per Million
CFU	Colony-forming units
ROS	Reactive oxygen species
CuTCPP-TSI	Copper (II)tetra (4- carboxyphenyl)porphyrin-sensitized titania-silica-iron oxide nanocomposites

Chapter 1
Introduction

1.1 Introduction to the research problem and significance

The presence of bacterial infection from *Escherichia coli (E. coli)* causes many infirmity symptoms in humans for instance cramps, diarrhea, nausea, etc. **[2]**. According to the World Health Organization (WHO), there were over 1 million of the population in the world during 2010 getting infections from foodborne Shiga toxin-producing *Escherichia coli* (STEC), and more than 100 of people were died from this *E. coli*. *E. coli* often contaminates the food and known as foodborne infection **[3]**, and it can appear in ruminant sources including cattle, sheep, goats and deer. Especially beef, it is often found 40% of STEC contamination in American cuisine **[4]**.

Furthermore, there were another important incident in Europe in 2011 where a large number of German populations were infected from verocytotoxin which were produced from *E. coli* causing the disease of bloody diarrhea and hemolytic uremic syndrome (HUS). Also, populations in other countries in Europe and North America were also inflected as well **[5]**.

Titania or titanium oxide (TiO$_2$) has ability on photocatalytic activities for bacterial effect, it can be used as antibacterial material for killing *E. coli*. In terms of medical application, titania becomes the most interested photocatalyst that utilizes ultraviolet light to activate bactericidal activities **[6]**. Titania not only has an excellent ability of photocatalyst, but it also presents a lot of its advanced properties such as low cost, high chemical stability, non-toxicity and resistance to other chemicals **[2]**.

Furthermore, the photocatalysis of titania has been reported to be a useful tool for wastewater treatment systems as well **[7]**. According to the studies, 15 percent of the synthetic dyes from the industrial activity like methylene blue(MB) are escaped from the industrialize areas into the aquatic environment **[8]** as these chemical substances contaminated the water source, it will also further flow into the surface water, groundwater and might be able to contaminate drinking water **[8, 9]**. Since titania photocatalysis is an effective method for applying wastewater treatment by producing reactive oxygen species (ROS) as strong oxidants that can oxidize organic compounds into biodegradable forms with lastly formation of a simpler product. **[10].**

However, as titania is insoluble in water which obstruct to separate and recover titania from the aqueous solution. Thus, in previous studies by our group **[1, 11]**, magnetic nanoparticles were applied to facilitate the separation process by being inserted as a core layer for responding with a

magnetic field. Among magnetic materials, iron oxide was selected as the most suitable material to use for this case because it is good for binding with antibiotics, excellent on biodegradability, and easy to prepare [12]. Moreover, there was a negative effect on photocatalytic activities from the interaction between titania and magnetic encouraging the recombination of photogenerated electron-hole pairs and lowering the efficiency to photocatalysis. In order to solve this problem, silica was inserted as an interlayer between iron oxide and titania due to the large band gap of silica, and enhancement in the photocatalytic activity was observed [11].

In the previous report from our research group, the ability of photocatalyst for bactericidal activities of titania-silica-magnetite nanocomposites was shown with promising results, but unfortunately it was able to produce in just a small (milligram) scale and was difficult to handle [1, 11]. Therefore, this project was conducted with a new synthesis method for fulfilling future real applications of large-scale production but maintain the same composition by designing the process to reach a gram-scale production. In this report, the nanocomposites of magnetic core covered by titania shell with silica as an interlayer ($Fe_3O_4@SiO_2@TiO_2$) was synthesized using co-precipitation and reverse microemulsion methods. The nanocomposites with varying amounts of silica interlayer were investigated as photocatalyst with a magnetically separable property based on their photocatalytic efficiency in degrading the methylene blue (MB). The best performance nanocomposites were further investigated for bactericidal activities using *E. coli* as a model.

1.2 Research objectives

This project aims to synthesize and characterize Titania-Silica-Iron oxide nanocomposites, as well as, to study their bactericidal activities toward *E. coli* based on their photocatalytic efficiency. Therefore, in order to achieve this project, there are following objectives:

1. To synthesize Titania-Silica-Iron oxide nanocomposites in a gram - scale

2. To identify the most suitable thickness of the silica of the nanocomposites based on their photocatalytic activity

3. To investigate the interaction of the Titania-Silica-Iron oxide nanocomposites with bacterial cells

1.3 Literature search

1.3.1 Magnetic nanoparticles

Magnetic nanoparticles are nanomaterials that express common characteristics in terms of nanoparticles but also magnetic properties as well. Nowadays, there are typically three forms of magnetic nanoparticle that are commonly used including metal, metal oxide, and metal alloy. These magnetic nanoparticles provide many important advantages on unique size and physicochemical property depending on various applications including biotechnology, biomedical, material science, engineering, and environmental areas. There are many benefits from the properties of magnetic nanoparticles including the surface effect, excellent biocompatibility, superparamagnetism, tumour thermotherapy, and ability of magnetic separation **[12]**. As magnetic nanoparticles in whether form of bare and modifying surface are present in terms of superparamagnetic which is especially appropriate to use in medical applications due to their excellent biocompatibility **[12, 13]**. Particularly, supermagnetic iron oxide nanoparticles have been widely utilized among diagnosis research of biomedical fields such as antibacterial activity as well **[12, 14]**.

1.3.2 Iron oxide nanoparticles

Iron oxide nanoparticles are inorganic nanoparticles which consist of maghemite (γ-Fe_2O_3) and/or magnetite (Fe_3O_4) particles with the dimension ranging between 1 to 100 nm. In nanoparticles, size and shape are critically important as it correlates with manufactures, processing, and applications of materials owing to the more surface area causing higher binding capacity and better dispersibility of nanoparticles in solutions **[15]**.

1.3.2.1 Applications

Mostly, iron oxide nanoparticles are considered to be the most significant usefulness in biomedical application including cell separation and detection, targeted drug delivery, and magnetic resonance imaging **[16]**. Nowadays, many researchers still work on their clinical investigation of MRI as therapeutic nanomedicine for cancer treatment by improving drug activity in combination therapy between iron oxide nanoparticle and chemotherapeutic drugs **[17]**.

1.3.2.2 Properties

The special property of iron oxide nanoparticle plays many important roles including low cost of production, non-toxicity to environment, stability, compatibility, excellent biodegradability,

low cytotoxicity, having capability for modifying with multiple substances, having capability for binding with multiple antibodies, and ease for preparation [12, 17].

1.3.3 Titania

Titania (TiO_2, titanium oxide or titanium dioxide) is white inorganic compound, which is normally made of ilmenite, rutile, and anatase minerals [18]. Titania are the most stable crystalline forms, at high temperature over 915 °C anatase can change to titania form [19]. Titania is very significant for industrial and daily life applications including photocatalytic environmental remediation procedures, gas sensors, pigments in paint, bacterial decontamination, and cleaning agent components [2, 18].

As titania nanoparticles have good ability on their photocatalytic activities due to inexpensive, high chemical stability, non-toxicity, insolubility in water, and resistance to other chemicals [2]. Titania photocatalysis could produce aqueous reactive oxygen species from ultraviolet light such as hydrogen peroxide, peroxyl radicals, superoxide and hydroxyl radicals (Figure 1) [20].
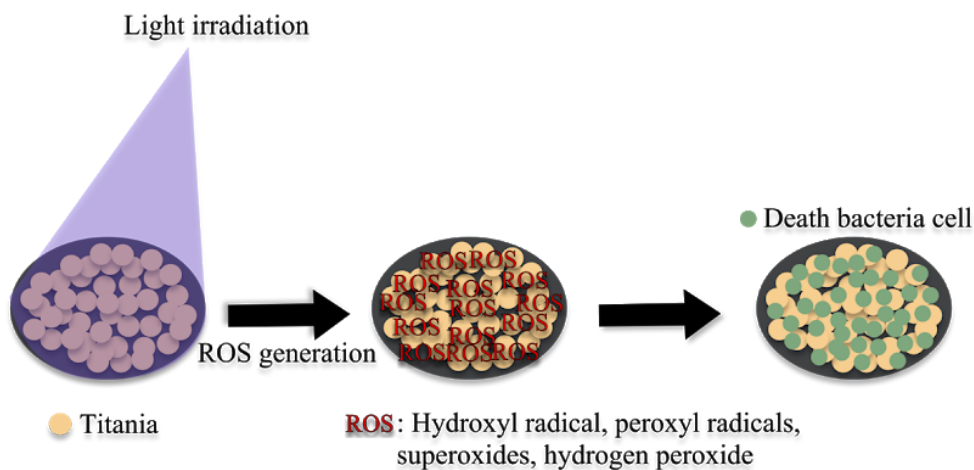
Figure 1. The scheme showing mechanism of reactive oxygen species (ROS) on the titania surface under light irradiation

According to antibacterial properties, photocatalytic titania provides a lot of benefits in terms of antibacterial. Firstly, titania has a wide range spectrum for bactericidal activity of Gram-negative and Gram-positive bacteria, fungi, and multidrug resistant straits. Secondly, titania is environmental safety since there is no toxic effect into the community. Lastly, titania nanoparticle coating works well for this case. The bactericidal activity from titania can be activated when photoexcitation upon exposure to UVA radiation in a range between 320 - 400 nm, which results in the production of extreme toxic reactive oxygen species (ROS), especially superoxide anion and

hydroxyl radicals. ROS are an important factor for killing bacteria as it generates a strong oxidative cell damage, which causes the leakage and destruction of intercellular continents in the cell [6, 21]. For instance, inhibition of cellular respiration by destruction of coenzyme A in cell membrane from ROS effect, also another the disruption of cellular metabolism by the effect from producing hydrogen peroxide [6]. Therefore, the photocatalytic titania can be proved to be an efficient method for bactericidal effect.

On the other hand, titania also has some disadvantages due to difficulty to separate and recover from aqueous solution [11]. To solve this problem, coating titania particles on the magnetic surface can lead to a magnetic separation. However, deposited metal oxides on titania surface could reduce photocatalytic performance due to an electron trap inducing electron-hole recombination. In order to prevent electron-hole recombination, which extends electron and hole in redox reaction, inserting some interlayers between the two materials were reported to help enhance photocatalytic activity [6, 11].

1.3.4 Silica

Silica or silicon dioxide (SiO_2) is a natural compound of silicon and oxygen which has three main crystalline phases including quartz, tridymite and cristobalite [22]. Due to the thermal stability and chemical inertness of silica, it is one of the most commonly used support materials in catalysis [23]. Also, silica has a large band gap, exhibits high thermal and chemical stability and has low toxicity [24].
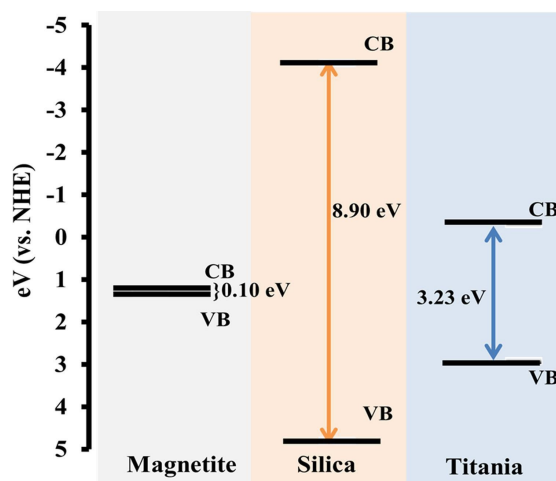
1.3.5 Titania-Silica-Iron oxide nanocomposites

Fig2ure 2. Band edge positions of magnetite, silica and titania [1]

Owing to the large band gap of silicon dioxide, it can act as a good insulating layer, so inserting a silica layer in between iron oxide and titania layer revealed a seriously higher in photocatalytic activities. The higher in photocatalytic activities due to the fact that the layer of silica prevents the electrons transfer between titania and iron oxide, and reduces the electron and hole recombination caused when two or more semiconductors are directly contact, in this case titania and iron oxide, as can be observed in Figure 2 **[2, 25]**.

1.3.6 *Escherichia coli* (*E. coli*)

Escherichia coli (*E. coli*) is a bacterium that is mostly found in the gut of human and warm-blooded animals, but it is normally harmless to humans. However, under some conditions, the bacteria can cause some health problems. For instance, foodborne disease is a disease caused by infection of Shiga toxin from E. coli O157:H7 (STEC). It can be transmitted into humans directly through food contamination such as raw meat products, raw milk, unclean raw vegetables and fruits. STEC can mature in temperatures ranging from 7 °C to 50 °C, but the optimum temperature that they favor to grow is 37 °C **[3]**.

1.3.6.1 Properties

E. coli is classified into the group of *Enterobacteriaceae* which is divided into six species composed of *E. coli, E. albertii, E. blattae, E. fergusonii, E. hermannii*, and *E. vulneris*. According to their morphology, *E. coli* are typically Gram - negative bacteria that have short rod-shape with the size at 0.5 μm ✕ 1-3 μm, which depend on their different of coccoid shape and long filamentous forms. They can be appeared to be in a single, pair, or in a short chain along with non-spore form. They use peritrichous for helping their movement **[26]**.

1.3.6.2 Symptoms

The symptoms of the disease that occur from *E. coli* is caused by the infection from STEC including abdominal cramps and diarrhoea. Bloody diarrhoea (hemorrhagic colitis) may also be another symptom if in case when the symptoms are in the progress. Fever and vomiting also show symptoms in this disease as well. However, the inflection of STEC can cause a life-threatening disease for instance haemolytic uraemic syndrome (HUS). There are 25% of HUS patients can get effects on their neurological complication, and another 50% of HUS survivors can gain side effects on their chronic renal sequelae **[3]**.

1.3.6.3 Sources and transmission

Mostly, the main reservoir of this STEC comes from animals, especially ruminant animals such as cattle, goats, and sheep **[27]**. Moreover, there are also found in some other mammals and birds. Then when humans consume these animal types as contamination food, STEC will be now transmitted into humans. In addition, during cultivation, vegetables and fruits can get contamination from STEC by contact with animals' feces as well. However, STEC can be also transmitted by infecting between human to human via oral and farce ways **[3]**.

1.3.6.4 Treatment

Antibiotics can be utilized to treat *E. coli* infection as it is the effective method to inhibit the growth of *E. coli*. Mostly, the common antibiotic agents for treating *E. coli* infection consist of β-lactams, fluoroquinolones, aminoglycosides and trimethoprim-sulfamethoxazole. Especially β-lactams antibiotics are the most crucial drug class for applying in this case **[26]**. However, antibiotics can be used when the symptoms are not too harsh. However, when the symptom is expressed with fever and bloody diarrhea, antibiotics should not be allowed to be used because of increasing the Shiga toxin production **[28]**.

Chapter 2
Experimental

2.1 List of Equipment and Instrument

2.1.1 X-ray Electron Diffraction (XRD)

X-ray electron diffraction (XRD) is a common technique that is used for characterization of core-shell nanoparticles, which is known as crystalline structure of materials [29]. The X-ray diffraction pattern is generated by constructive interference of a monochromatic beam of X-rays as it was scattered from the set of lattice planes of sample at each specific angle. Therefore, the coherent scattering of photons forming X-ray beams helps to interpret the information on the crystalline structure of the sample including structures, phases, texture, and other structural parameters. Moreover, XRD also provides the peak intensities by distribution of atoms in the lattices [30]. According to this experiment, XRD was used to define the crystallinity and the structural chemical compositions of the material correlate with the reference peaks from the database.

2.1.2 Scanning Electron Microscopy (SEM)

Scanning electron microscopy (SEM) is a type of electron microscope. It is utilized for characterizing the material from nanometer to micrometer size which can be scanned and gives out an image of a sample by beam of electrons. When the electrons interact with atoms in the surface region of the sample, it will generate some signal as secondary electrons in the composite. The intensity of secondary electrons will be used to compare with the scanned electron beam that expresses the image of the composition and surface topography of the sample [31]. In this experiment, SEM was applied to examine chemical composition and 3-dimensional surface morphology of the material.

2.1.3 Transmission Electron Microscopy (TEM)

Transmission Electron Microscopy (TEM) is the most useful type of electron microscopy for characterization nanomaterial since it is easy for sample preparation and comprehension of image. TEM uses a high electron beam to shoot with the atoms of a sample, and this interaction activates the signal to form an image. Therefore, TEM provides a better level of atomic dimension with higher resolution image and higher analytical measurement than SEM [7]. In this experiment, the TEM was used to see the internal structure, shape and size of the material.

2.1.4 UV-Visible Absorption Spectroscopy

UV-vis Absorption Spectroscopy is a primary instrument for the quantitative analytical technique focusing on the absorption in ultraviolet visible spectral regions by the chemical species in solution. The electromagnetic spectrums in these regions provide energy and make electronic transitions to occur, which refers to the excitation of electrons from ground state to the higher energy states **[32, 33]**. According to this experiment, the HP 8453 (Agilent, USA) UV-vis spectrophotometer was used to evaluate the photocatalytic activity of each prepared sample. The absorbance of each prepared sample was measured with the fixing wavelength at 664 nm and 800 nm.

2.1.5 Laboratory Instruments

According to this statement, the laboratory instruments were used for preparing all the sample in step of synthesis of Titania-Silica- Iron oxide nanocomposites, characterization, photocatalytic degradation measurement, and bactericidal activity which are listed below (Table 1):

Instrument	Synthesize the material	Characterization	Photocatalytic degradation	Bactericidal activity
1. Glass Beaker	✔	✔	✔	✔
2. Erlenmeyer Flask	✔		✔	✔
3. Petri dish		✔		✔
4. Syringe	✔			
5. Micropipettes	✔	✔	✔	✔
6. Round bottom flask	✔			✔
7. Crucibles	✔			
8. Mortar and pestle	✔	✔		

9. Measuring cylinders	✓		✓	
10. Dropper	✓			
11. Glass stirring rod	✓			
12. Sonicator	✓	✓	✓	✓
13. Rotary evaporator	✓			
14. Cuvette			✓	
15. Separatory funnel	✓			
16. Glass vial	✓	✓	✓	
17. Reflux apparatus	✓			
18. Magnetic retriever	✓			
19. Magnetic stirrer	✓		✓	
20. Magnetic stir bar	✓		✓	
21.Magnetic decantation	✓			
22. Bacterial culturing test tubes				✓
23. Centrifuge tube				✓
24. Incubator				✓
25. Shaker				✓

Table 1. The list of Laboratory Instruments

2.2 List of chemicals and materials

The Titania-Silica-Iron Oxide Nanocomposites was synthesized for antibacterial agent by using the following chemicals: Iron (III) chloride hexahydrate ($FeCl_3.6H_2O$), Iron (III) sulfate hexahydrate ($FeSO_4.7H_2O$), Tetrabutyl orthotitanate (TBOT), Tetraethyl orthosilicate (TEOS), 1-Hexanol, Methylene Blue hydrate, Hexadecyltrimethylammonium bromide ($C_{19}H_{42}BrN$, CTAB), Titanium(IV) butoxide purchased from Sigma-Aldrich chemical, USA. Sodium hydroxide (NaOH) and Ammonia solution 25% were purchased from MERCK, Germany. Ethanol (C_2H_5OH) was purchased from RCL Labscan Limited, Thailand and Milli-Q water.

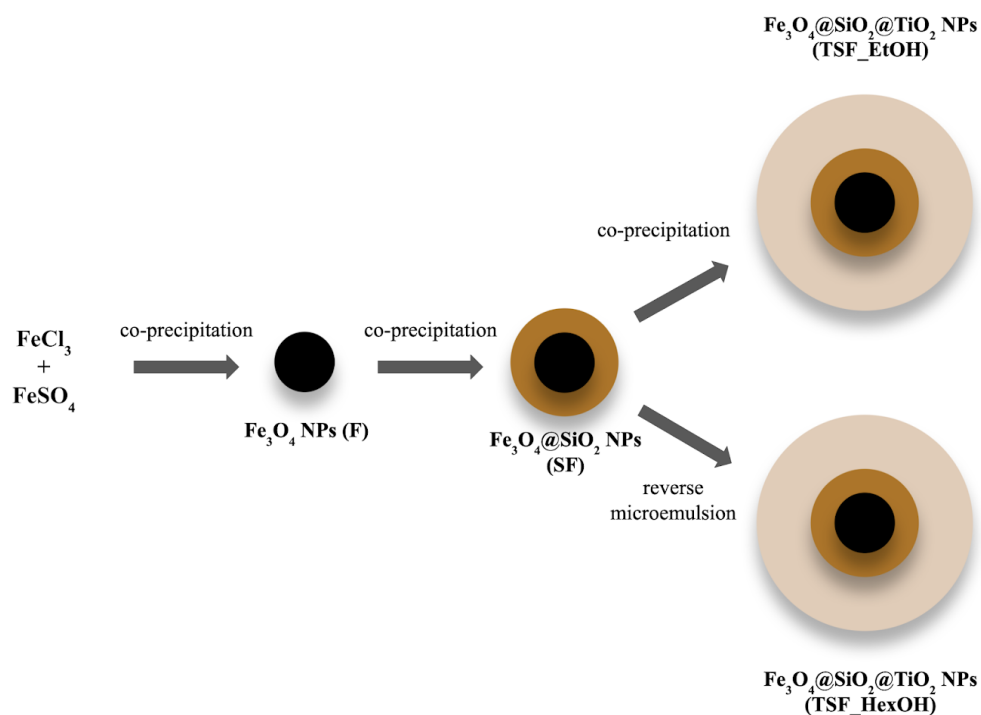## 2.3 Experimental procedure

2.3.1 Synthesis of material

Figure 3. Scheme for the synthesis of $Fe_3O_4@SiO_2@TiO_2$ magnetic nanocomposites

2.3.1.1 Synthesis of magnetic ferrite nanoparticle (Fe_3O_4)

The magnetic ferrite nanoparticles were synthesized by co-precipitation method. Firstly, 0.51g of $FeCl_3.6H_2O$ and 0.54g of $FeSO_4.7H_2O$ were prepared in 150 mL of Milli-Q water as precursors. After that, the mixture of precursors was set to reflux at 70 °C and kept stirred at 650 RPM. While the mixture was undergoing the refluxing, NaOH was slowly added dropwise using a syringe until the solution had a value of pH ranges between 10 to 11. During the addition of NaOH, the reaction occurs and causes the formation of brown precipitation. After NaOH was added, the solution then maintained refluxing for 2.5 h. The product was then separated by magnet decantation and washed three times with milli-Q water and another three times with ethanol. Finally, the product was being dispersed in ethanol for further use.

2.3.1.2 Synthesis of $Fe_3O_4@SiO_2$ Microspheres

The synthesis of silica-coated iron oxide nanoparticles was prepared using the reverse microemulsion method. First of all, 0.1 g of the prepared Fe_3O_4 was added into a mixture solution

composed of 80 mL of ethanol and 20 mL of milli-Q water. Then, tetraethyl orthosilicate (TEOS) and Ammonium hydroxide solution ($NH_3.H_2O$) was added (the molar ratio of TEOS: $NH_3 \cdot H_2O$ = 3:4) while the resulting solution was vigorously stirred at room temperature for 24 h. After 24 h, the silica-coated iron oxide nanoparticles were collected and separated by magnetic decantation, washed repeatedly with three times of milli-Q water and three times of ethanol. Finally, the product was dispersed in ethanol.

According to the preparation of silica-coated iron oxide nanoparticles, the amount of TEOS that was added as silicon source was varied to observe by the thickness effect of silica coated on iron oxide nanoparticle surface. There were various amounts of TEOS which were added to the above mixture solution including 37.5, 150, 600, and 900 µL per 0.1 g of Fe_3O_4.

2.3.1.3 Synthesis of $Fe_3O_4@SiO_2@TiO_2$ Microspheres

In this project, titania was coated onto the $Fe_3O_4@SiO_2$ Microspheres by using two methods including reverse microemulsion method and co-precipitation method. Each method was different by the solvent that was used, which are hexanol and ethanol. Hence, the effect of distinct solvent would be further investigated.

Following the reverse microemulsion method was used hexanol as a solvent for the synthesis of titania coating on silica iron oxide surface. Specifically, 0.1 g of silica-coated iron oxide nanoparticles was dispersed into a solvent of 7.3 mL of 1-hexanol. Then, 3g of cetyltrimethylammonium bromide (CTAB) and 1 mL of milli-Q water were added to solution of silica-coated iron oxide containing 1-hexanol solvent, the mixture was stirred until CTAB was well mixed and dissolved. Subsequently, the mixture solution was continually added with 1250 µL of tetrabutyl orthotitanate (TBOT), vigorously stirred and refluxed at 80°C for 24 h. The product was then collected and washed using magnet decantation or centrifuge with two times of 1:1 volume ratio of ethanol: milli-Q water and another time with ethanol. Finally, the final product of titania-silica-iron oxide nanocomposites was re-dispersed in ethanol.

On the other hand, in the co-precipitation method, ethanol was used as a solvent to coat titania on the silica iron oxide surface. Briefly, 0.1 g of silica-coated iron oxide nanoparticles was prepared in solution of 41.483 mL of ethanol and 0.891 mL of milli-Q water. Then, the diluted TBOT was separately prepared by dissolving 1250 µL of tetrabutyl orthotitanate (TBOT) in 2.965 mL of ethanol. The diluted TBOT was then gently added into the solution while stirring and set the reflux at 90 °C for 2 hours. The product was then separated and washed by magnet decantation or centrifuge with two times of 1:1 (ethanol: Milli-Q water) and once with ethanol. Consequently, the

final precipitation of titania silica iron oxide nanocomposites was dried in an oven at 100 °C for 12h, and then finally calcined in the box furnace at heat 500 °C for 2h. In this experiment, the different conditions of Titania-Silica-Iron oxide nanocomposites were prepared by the following Table 2.

Sample #		Iron oxide (g)	Silica (TEOS) added (µL)	Titania (TBOT) added (µL)	Solvent Used	Method for coating titania
A	1250TS150F_HexOH	0.1	150	1250	Hexanol	Reverse microemulsion
B	125TS150F_EtOH	0.1	150	125	Ethanol	Co-precipitation
C	375TS150F_EtOH	0.1	150	375	Ethanol	Co-precipitation
D	1250TS37.5F_EtOH	0.1	37.5	1250	Ethanol	Co-precipitation
E	1250TS150F_EtOH	0.1	150	1250	Ethanol	Co-precipitation
F	1250TS600F_EtOH	0.1	600	1250	Ethanol	Co-precipitation
G	1250TS900F_EtOH	0.1	900	1250	Ethanol	Co-precipitation
H	1250T_EtOH	-	-	1250	Ethanol	Co-precipitation

Table 2. The name lists of different material of Titania-Silica-Iron oxide nanocomposites

2.3.2 Characterization methods

2.3.2.1 X-ray Electron Diffraction (XRD)

To determine the structure and crystalline properties of Titania-Silica-Iron Oxide nanocomposites, XRD was performed by using D/MAX 2200 X-ray diffractometer (Rigaku, Japan) through Cu-Kα radiation with accelerating voltage and an applied current of 40 kV and 30 mA. The intensity was settled at 2θ in a range of 20°– 90°.

2.3.2.2 Scanning Electron Microscopy (SEM)

The morphology and chemical analysis of Titania-Silica-Iron oxide nanocomposites were characterized using JEOL (JSM-IT 100).

2.3.2.3 Transmission Electron microscopy (TEM)

The TEM image was recorded using Philips TECNAI 20 transmission electron microscope at the accelerating voltage of 120 kV. The sample was prepared by dispersing a little amount of the sample powder in ethanol and letting the dispersion well mixed by applying an ultrasonic treatment for 10 mins. The dispersion was then dropped on a Formvar-coated copper grid and dried at room temperature to be ready for TEM measurement.

2.3.3 Photocatalytic degradation measurement

The photocatalysis of the synthesized magnetic nanocomposites were measured using the HP 8453 (Agilent, USA) UV-vis spectrophotometer. The samples that were tested for the photocatalytic activity are Fe_3O_4, 1250Titania_EtOH (Sample H), 1250TS150F_HexOH (Sample A), 1250TS37.5F_EtOH (Sample D), 1250TS150F_EtOH (Sample E), 1250TS600F_EtOH (Sample F), and 1250TS900F_EtOH (Sample G). This experiment was conducted under room temperature by irradiating 20 W of WSFSWL blue UV blacklight onto each of the prepared samples in a beaker that were dispersed in the 30 mL of 10 ppm methylene blue. In each of the beakers, ⅛ or 0.125 batches (0.0250 g of Fe_3O_4, 0.3833 g of 1250Titania_EtOH, 1.3 mL of 1250TS150F_HexOH, 0.0508 g of 1250TS37.5F_EtOH, 0.4221 g of 1250TS150F_EtOH, 0.0462 g of 1250TS600F_EtOH and 0.0439 g of 1250TS900F_EtOH) of synthesized nanocomposites were used at a time. Each of the samples were collected from 0 to 5 h at 0, 0.5, 1, 1.5, 2, 3, 4 and 5 h where the first state of collecting was started at 1 h after stirring the solution of samples. The blacklight was irradiated after the first time of sample collection. During the irradiation of blacklight, the beakers were kept away from other light sources and being stirred continuously.

2.3.4 Bactericidal activity

Bacterial cells of *E. coli* were prepared by aerobic maturing into 5 mL of Luria-Bertani (LB) broth and cultured overnight at 37°C with shaking at 150 RPM for 2.5 h in a shaking incubator. The culture of *E. coli* was isolated into a fresh LB broth and grown until reaching 600 nm at 0.5 of optical density. The exponential phase cells were centrifuged for 10 min for ready collecting at 25 mL of each and resuspending in sterized normal saline of 0.9% sodium chloride. The suspension of bacterial cells was treated in different concentrations of 0, 32 and 50 mg Titania-Silica-Iron oxide nanocomposites by lighting up at 37°C for 3h with 100W incandescent lamp. The survival cells could be carried out from the colony by counting after irradiation through a viable cell count method. Moreover, bacterial cells would be incubated at 37°C for 3h, then colony-forming units

(CFU) were counted. However, the control experiment in this case was conducted by controlling the bacterial cells, which were treated and without treated with activated UV light.

Chapter 3
Result & Discussion

In this experiment, the final product of Titania-Silica-Iron oxide nanocomposites was eventually synthesized in the form of brown precipitation, allowing rapid capture and removal by attraction from magnetic fields. However, using the assistance of magnetic attraction to separate out the product may wash some of them away, so the product was not completely collected. This brown precipitation was formed in delicate powder for further used. The way for synthesis of these Titania-Silica-Iron oxide nanocomposites in large gram - scale was repeatedly produced for four times with the final product yields approximately at 0.4816 ± 0.1309 g/ batch, in which each batch was containing 0.1000 g of magnetite. In comparison, the previous work [1] was generated around 0.1005 ± 0.01140 g/ batch with repeating two times for synthesis of the product, which is less than the product generated from this experiment.

3.1 Characterization of nanocomposites

3.1.1 XRD patterns

From the XRD patterns of the crystal structure of Titania-Silica-Iron oxide nanocomposites with varying amounts of silica added from co-precipitation method, anatase titania and magnetite phase were identified as shown in Figure 4. The reference peaks for magnetite phase and anatase titania are marked with "M" and "T", respectively. As shown in Figure 4, there are 5 patterns of different amounts of TEOS used, which include 37.5, 150, 600 and 900 μL. According to the XRD pattern of iron oxide nanocomposites shown in Figure 4b, it shows the sharp peaks at 2θ ranges between 20°-80° matched the reference pattern of magnetite phase. Also, anatase titania's pattern in Figure 4a shows the strong peaks corresponding to its reference pattern. As shown in Figure 4c-g, all five the diffraction patterns of Titania-Silica-Iron oxide nanocomposites with varying amount of added TEOS reveals the combination characteristic diffraction peak of both magnetite phase and anatase titania as compared with their reference diffraction peaks. In conclusion, the XRD analysis gives the information to confirm that the synthesized titania-silica-iron oxide nanoparticles of different amounts of TEOS added contained magnetite and anatase as needed.

Alternatively, the XRD patterns in Figure 5 show the comparison between two diffraction patterns of Titania-Silica-Iron oxide nanocomposites with the same amount of added silica, but different in the synthesis methods, co-precipitation method and reverse microemulsion method. As

shown in Figure 5, the diffraction pattern of the Titania-Silica-Iron oxide nanocomposites using co-precipitation method (Figure 5b) exhibits sharper peaks that are clearly seen when compared with the one using reverse microemulsion (Figure 4a). Therefore, it can be implied that using a co-precipitation method can produce the composites with more intense magnetite and, especially, anatase titania peak as well as its higher crystallinity which can lower the band gap energy of anatase titania resulting in easier to generate the radicals. As synthesized using the reverse microemulsion method required surfactant to be used, the size and shape of the particle has been controlled due to its smaller crystallite size and less intense diffraction peaks [34]. On other hand, in this experiment synthesizing using co-precipitation method require to treat the nanocomposites with heat at 500°C in order to change titania from amorphous to anatase phase which created larger crystallite size owing to more intense in diffraction peak compared with reverse microemulsion method [35].
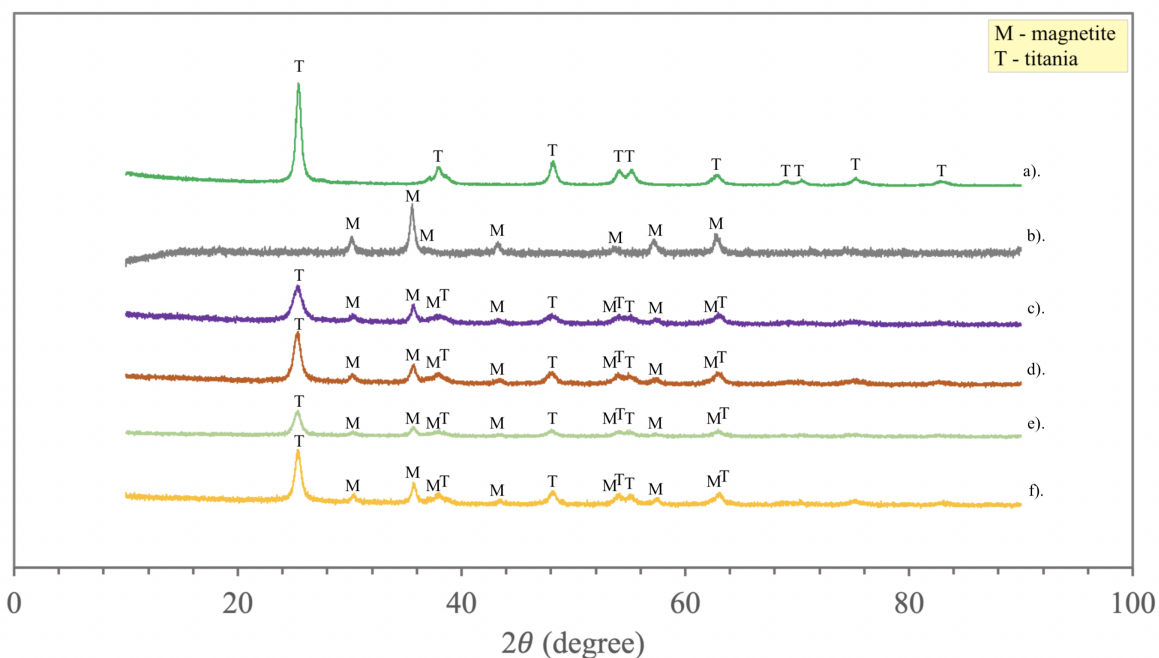

Figure 4. X-ray diffraction patterns of a). Titania, b). Magnetite, c). 1250TS37.5F_EtOH, d).1250TS150F_EtOH, e). 1250TS600F_EtOH, f). 1250TS900F_EtOH
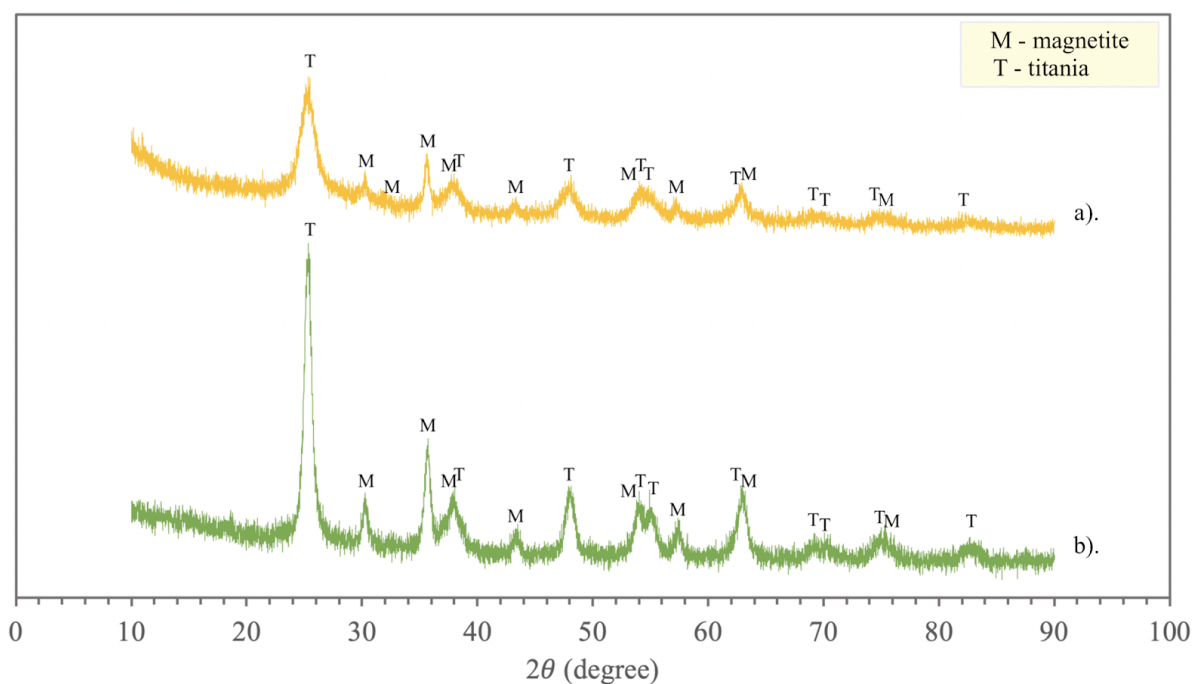
Figure 5. X-ray diffraction patterns comparing between a). 1250TS150F from reverse microemulsion method and b). 1250TS150F from co-precipitation method

3.1.2 SEM

The morphology and structure of nanocomposites with different thickness of silica layers and solvents were studied using SEM.

The SEM photographs of 1250TS150F_EtOH (Sample E) as shown in Figure 6a-b expressed the structure of particles with spherical shape and ellipsoidal morphology with agglomerates between the particles, the diameter range was approximately 0.214 to 0.521µm as displayed in Figure 6c. According to Figure 7, the EDX elemental maps of these nanocomposites consisted of oxygen, silica, titanium, and iron oxide, which showed completely formation of all particles that had coated onto the material for each layer. Due to the presence of oxygen, the oxygen peak created by responding of SiO_2.

As shown in Figure 8, 1250TS600F_EtOH (Sample F) (Figure 8a-b) also displayed the structure with the sizes of spherical shape and some with semi-spherical shape ranging from 0.149 to 0.456 µm and the size average of 0.307 µm (Figure 8c). As compared to sample E, the amount of silica added for sample F (Figure 8a-b) was higher than sample E at 450 µL, but both particle sizes seemed similar to each other. Due to non-controlled initial particle size of iron oxide, the particle size might cause board distribution of sizes before coating silica layers. Besides, following the EDX test of the sample F presented all the elements for preparing the nanocomposite including oxygen,

silica, titanium and iron oxide as indicated on Figure 8d, 9. Hence, Because of the increasing amount of silica added in sample F, the mass percentage of silica layer in this material was also higher than sample E by approximately 1.64% (Table. 3), which could prove that the silica was really coated on the material surface although the particle size between sample E and sample F similar by the size analysis from SEM images.

Figure 10 represented the SEM micrographs of 1250TS150_HexOH (sample A) (Figure 10a-b), whose shape wasn't clear enough to explain in this case as the particles were polydisperse from each other. The size range of sample A was 0.148 to 0.597 µm with the average of 0.257 µm in diameter (Figure 10c). This reason might be explained due to the experimental procedure in this nanocomposite with hexanol solvent, which did not require the precedence calcination step as in the ones that used ethanol as a solvent. Since Sample C and Sample F were specially required calcination at 500°C, the high temperature from calcination could cause the particle to change from amorphous to anatase and also increased the size of particles [36]. Furthermore, calcination also made titania to be a higher crystallization as a result important factor for improving the ability of the photocatalytic activity as well [37]. On the other hand, for hexane was already stated in anatase phase, it did not require to work on the calcination process, and the particles were originally already formed in a smaller size than ethanol ones [38]. In addition, since the method of using ethanol solvent was costless in terms of surfactant used than the ones using hexanol solvent due to non-additional requirement for using CTAB. Thus, this reason also could be described why hexanol was not efficient to use in this experiment. Following EDX analysis (Figure 10d, 11), oxygen, silica, titanium and iron oxide appeared in the formation of the nanocomposite of Sample A as well.
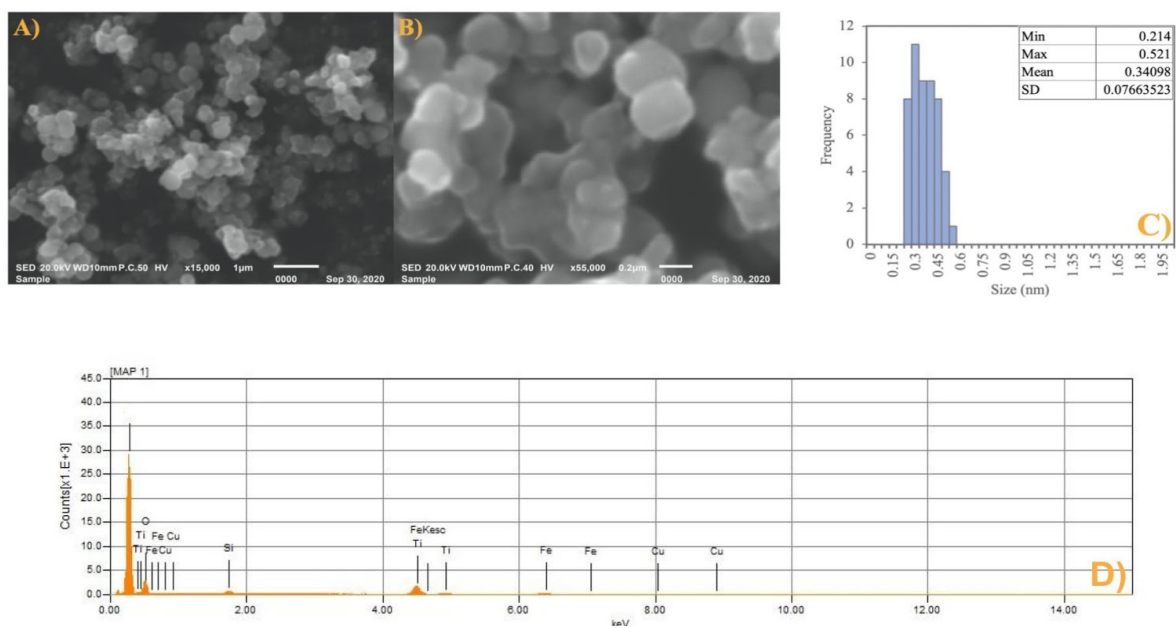
Figure 6. a-b). The SEM images of sample E, c). Particles size distribution histogram of sample E, and d). EDX analysis of sample E **(1250TS150F_EtOH)**

Figure 7. EDX elemental maps of Ti, Si, Fe, and O for Sample E

Figure 8. a-b). The SEM images of sample F, c). Particles size distribution histogram of sample F, and d). EDX analysis of sample F **(1250TS600F_EtOH)**

Figure 9. EDX elemental maps of Ti, Si, Fe, and O for Sample F

Figure 10. a-b). The SEM images of sample A, c). Particles size distribution histogram of sample A, and d). EDX analysis of sample A **(1250TS150F_HexOH)**
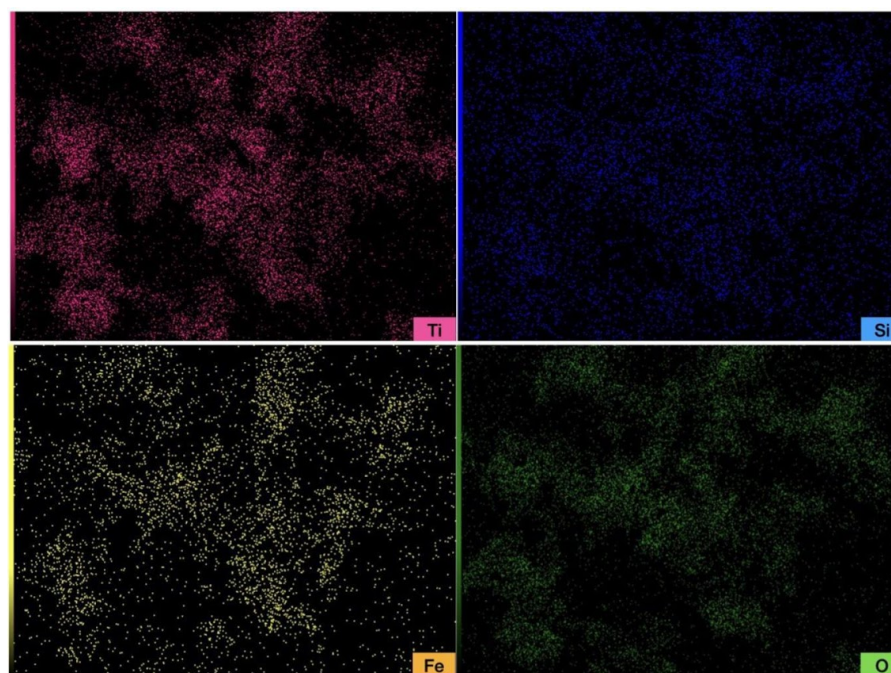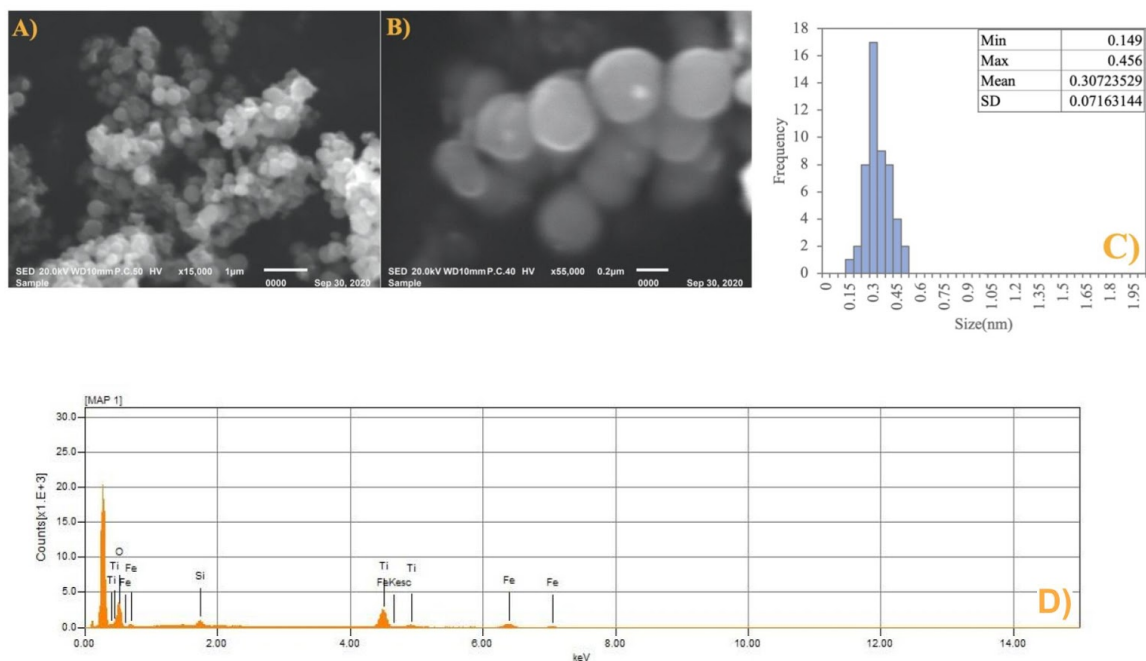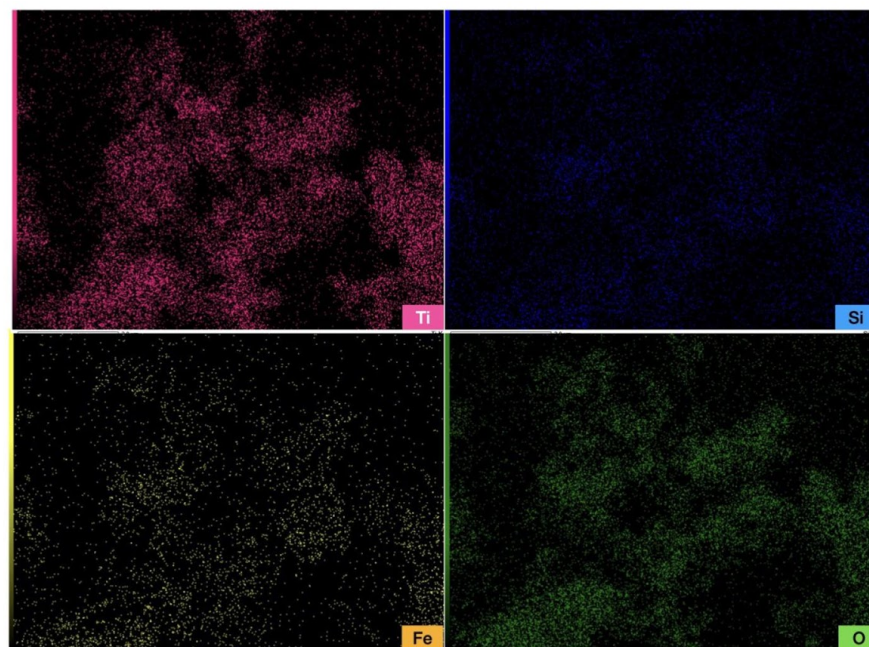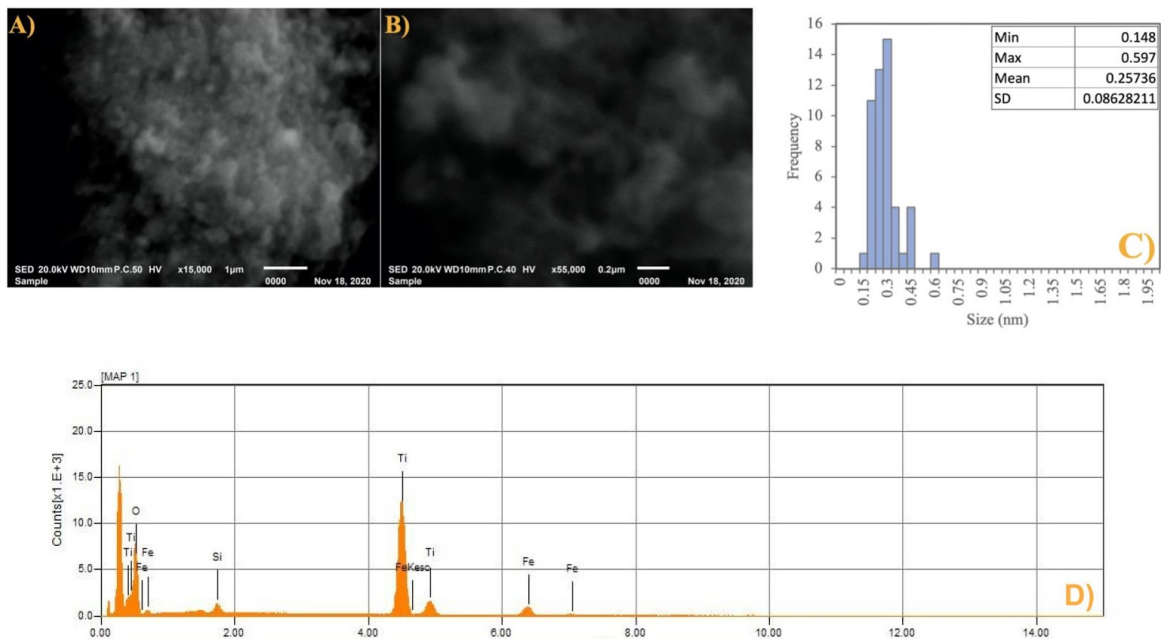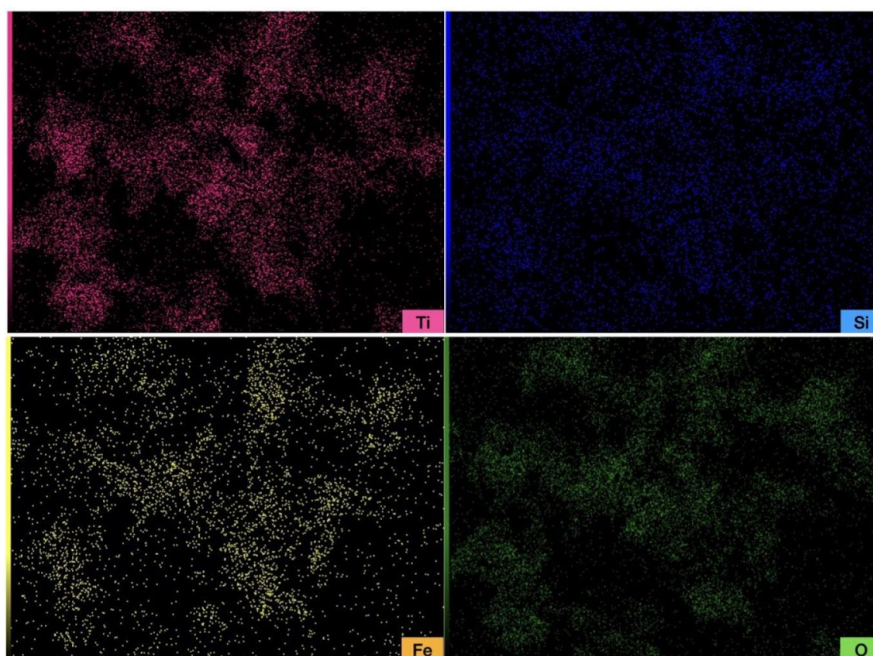

Figure 11. EDX elemental maps of Ti, Si, Fe, and O for Sample A

Mass %	Ti	Si	Fe	O
Sample E (1250TS150F_EtOH)	26.73	2.31	9.54	61.43
Sample F (1250TS600F_EtOH)	27.28	3.95	10.36	58.41
Sample A (1250TS150F_HexOH)	40.17	1.14	6.28	52.14

Table 3. Mass percentage of Ti, Si, Fe, O for EDX analysis of Sample E, Sample F, and Sample A

3.1.3 TEM

The morphology and sizes of the three as-prepared samples including iron oxide nanoparticles, iron oxide nanoparticles coated with silica using 600 µL TEOS and titania-silica-iron oxide nanocomposites with 600 µL TEOS (Sample F) were observed using transmission electron microscope or TEM. As shown in Figure 12, the sizes of the prepared sample and the layer of the particles can be defined from these TEM images. According to Figure 12a, from the observation, the iron oxide nanoparticles can be seen in spherical shape, even though the particles are not quite well-dispersed. The particle diameters are ranging from around 8.336 to 30.204 nm with the average sizes of 13.848 ± 4.153 nm, according to Figure 12b, which the diameter size seems to be bigger and has a wider size distribution when compared to the iron oxide nanoparticles prepared by P Chanhom et al. [1]. However, the reason why the particle size is larger might be the difference in synthesis method as P Chanhom et al. [1] was using thermal decomposition method differ from this experiment which was using co-precipitation method since it is easier to conduct, less harmful and better suited for large scale production [39]. After the silica was coated on the iron oxide nanoparticles, the particles were aggregated together as shown in Figure 12c-d, their size ranges from 11.951 to 40.038 nm and have an average size of 18.966 ± 4.984 nm. Furthermore, the silica shells of the particles were observed as a light grey layer surrounding the iron oxide (Fe_3O_4) core (dark grey), which can reveal the existence of $Fe_3O_4@SiO_2$ core/shell structure. The TEM image of titania-silica-iron oxide nanocomposites (600 µL TEOS) in Figure 12f shows some of the agglomeration between particles in which the average particle size is 159.9 ± 29.578 nm. However, the layers of titania are not clearly seen as it can be proposed that the titania layer was too dense to

be clearly shown in TEM corresponding to the weight percentage of titanium from the SEM (Table. 3) that shows a high amount. However, the existence of titania can be confirmed from EDX elemental analysis (Figure 8) and the particle size became bigger after coated with titania. Additionally, in accordance with Figure 12e, the thickness of the silica layer of the nanocomposites were measured, and the result came out that the average thickness is around 3.764 ± 0.856 nm.
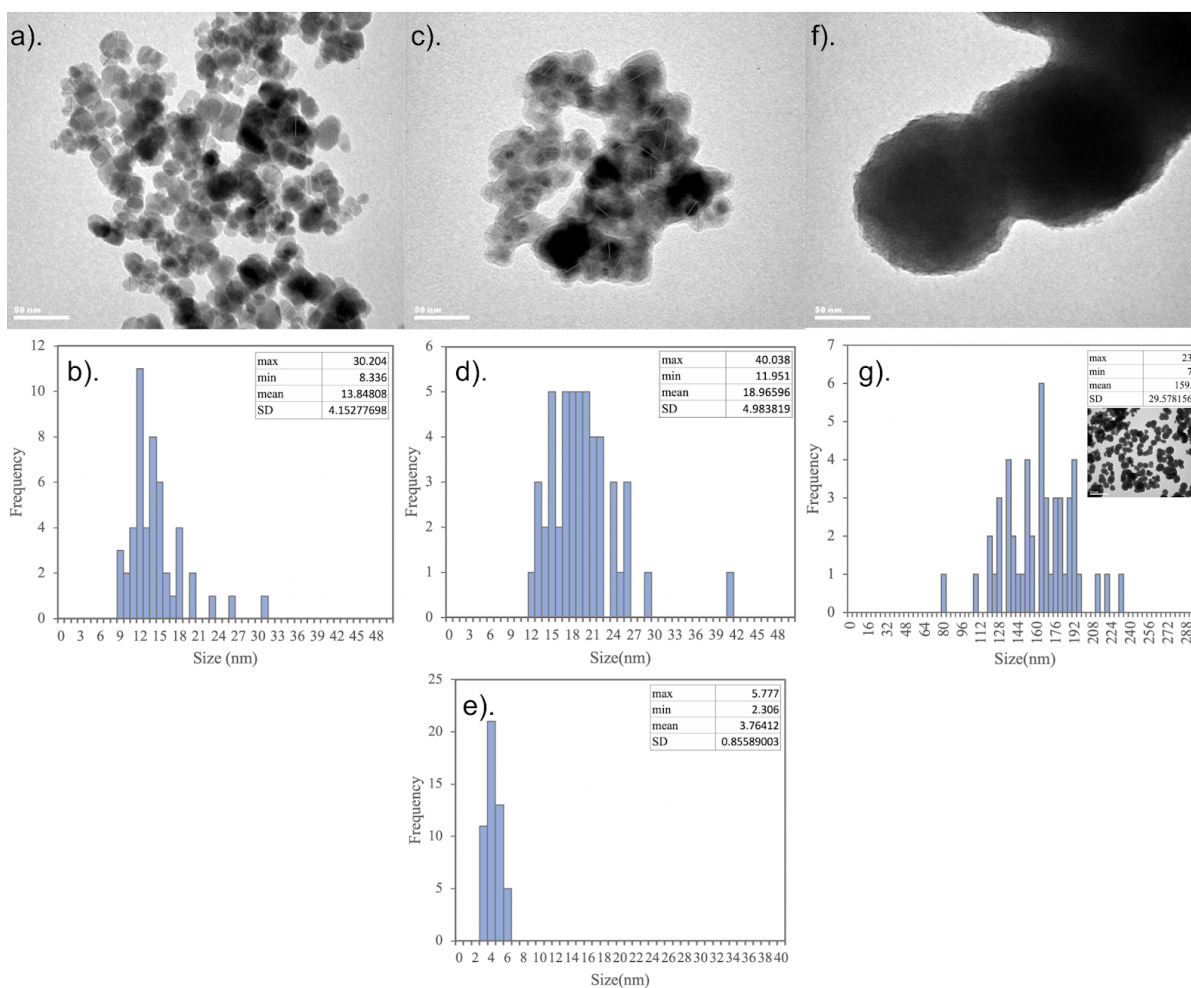
Figure 12. The TEM images and particles size distribution histogram from each layer of 1250TS600F (Sample F) including a-b). magnetite nanoparticles, c-d). $Fe_3O_4@SiO_2$ nanocomposites, e). silica layers, f-g). $Fe_3O_4@SiO_2@TiO_2$ nanocomposites

3.2 Photocataytic activity

To compare the efficient photocatalytic activity, methylene blue was utilized to study photocatalyst under UV irradiation.

In this experiment, firstly, the degradation of nanocomposites with coating of 150 µL of silica layer in the two solvent systems, hexanol and ethanol, was investigated. The nanocomposites

in the hexanol solvent and ethanol solvent were prepared by reverse microemulsion and co-precipitation methods. Following Figure 13, the nanocomposite with ethanol solvents had displayed a greater photocatalytic activity ability than the one that used hexanol as a solvent. Following the XRD result, as the one using co-precipitation method was shown to has a more intense diffraction peak of anatase titania which could prove that it has a higher crystallinity than the one using reverse microemulsion method, this could be explained by the lowering of band gap energy which require less energy to generate radicals to activate photocatalytic activity occurred. The synthesis of titania shell in this case did not affect photodegradation activity based on the percentage of photocatalytic activity. However, the co-precipitation method is selected to be the most comfortable to prepare and low cost, since CTAB didn't require it to be used in this method. Thus, ethanol is the best solvent for applying photodegradation in this experiment, so that is why ethanol will be decided and held for the entire of this project.

Next, there were three materials which were different by the amount of titania shell added as shown in Figure 14 with the comparison to the nanocomposites reported in P Chanhom et al [1]. At first the TBOT were added at 125 µL, but the photocatalytic result was shown to be at 11.27 % ± 19.53, which is still too low to work as a catalyst. Then we continued to add up the titania layer with 375 µL TBOT, but the result still did not differ from the first one at about 4.45%. Next 1250 µL TBOT were finally decided to select as the best amount of titania added since the degradation is dramatically increased higher than the last two thinner shells (~75.36 %). This indicated that when more and more of titania added, there will be more photocatalytic activity. For this reason, 1250 µL of TBOT were used at the exact amount in nanocomposites for the entire of this experiment.

Then, photocatalytic activity was used to investigate the effect of the quantity of silica layers on the material surface. According to Figure 15, photocatalytic activity was compared with various amounts of silica layer including 37.5, 150, 600, and 900 µL. In these four catalysts, Sample F provides the highest efficiency on their photocatalytic activity as the percent degradation of methylene blue was 97.65 ± 0.96 % in 5 h under irradiation, while the others show photocatalytic activity under the same condition in following order, Sample G > Sample E > Sample D. However, since the percent degradation of sample F was different from sample G just about 3.97 % ± 2.79, which did not seem too different within the error bar between these two. Furthermore, inserting silica as an interlayer between magnetic and titania would help to reduce electron-hole recombination occurred during generating absorbed species in photocatalytic activity as silica had a larger band gap than titania and magnetic. Furthermore, inserting silica as an interlayer between magnetic and titania would help to reduce electron-hole recombination occurred during generating absorbed species in photocatalytic activity as silica had a larger band gap than titania and magnetic.

Therefore, these results showed that the more thickness of the silica layer significantly improved the photodegradation efficiency of Titania-Silica-Iron oxide nanocomposites.

Moreover, as in Figure 16, the various types of materials that composed in the nanocomposites were used to study the photocatalytic activity efficiency which consists of titania, nanocomposite, and magnetite. The photocatalytic activity of Sample F (1250TS600F_EtOH) was observed to be the most efficient materials showing 97.65 % ± 0.96 of degradation, while titania and magnetite had the percent degradation of 83.35 % ± 1.03 and ± 0.74 % ± 1.19, respectively. According to the previous research, if there is no silica layer insert between titania and magnetite, it will cause electron hole recombination as titania produces some radical during the activated from UV light irradiation, so this will affect to titania's ability to degrade in methylene blue [40]. It could be concluded that the ability of titania or magnetite when working alone as a photocatalyst was not as efficient as the nanocomposites.
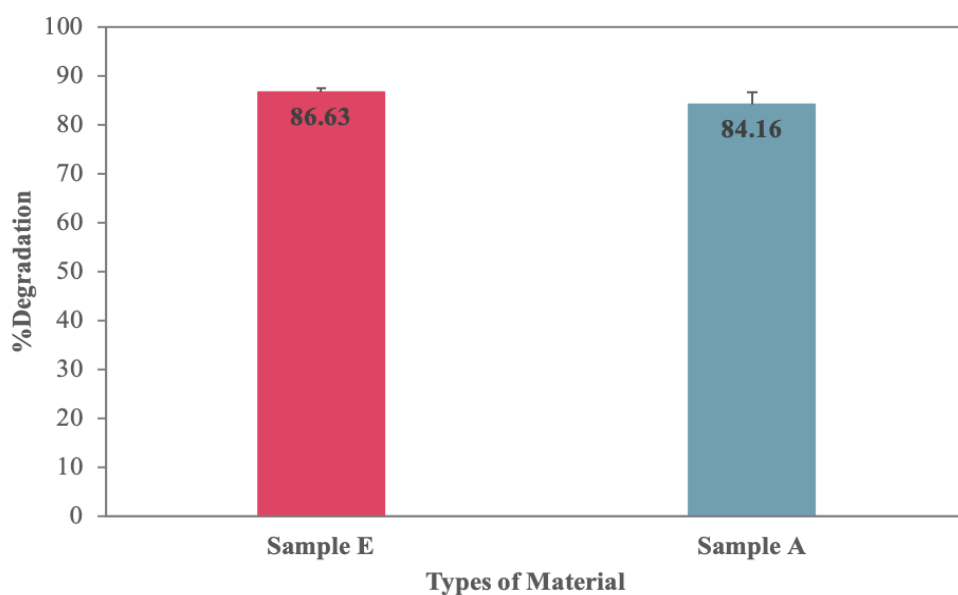

Figure 13: Comparison of photocatalytic degradation of two samples with different solvents used: 1250TS150F_EtOH (Sample E), 1250TS150F_HexOH (Sample A)

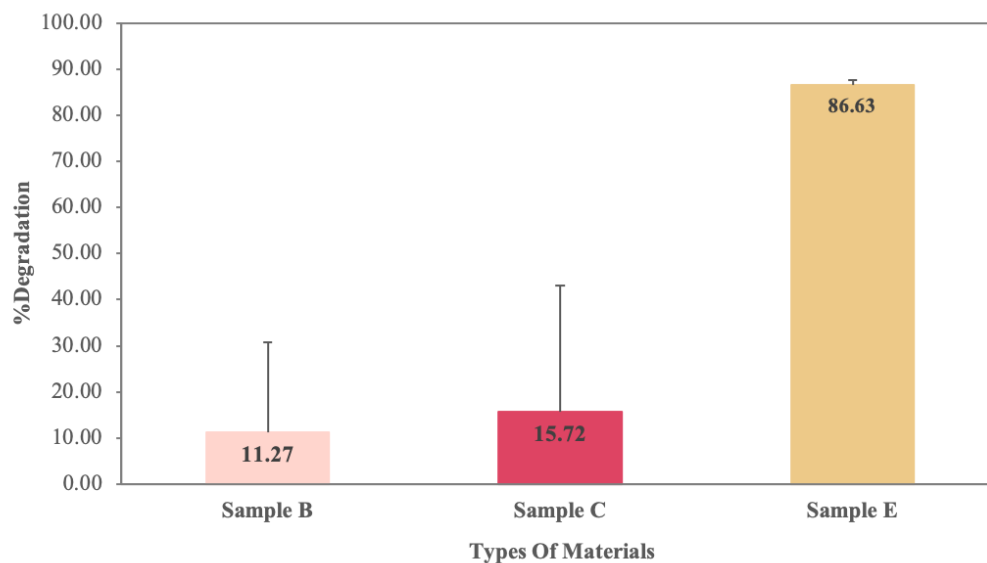**Figure 14.** Comparison of photocatalytic degradation of four samples with different amounts of titania added: 125TS150F_EtOH (Sample B), 375TS150F_EtOH (Sample C), 1250TS150F_EtOH (Sample E)
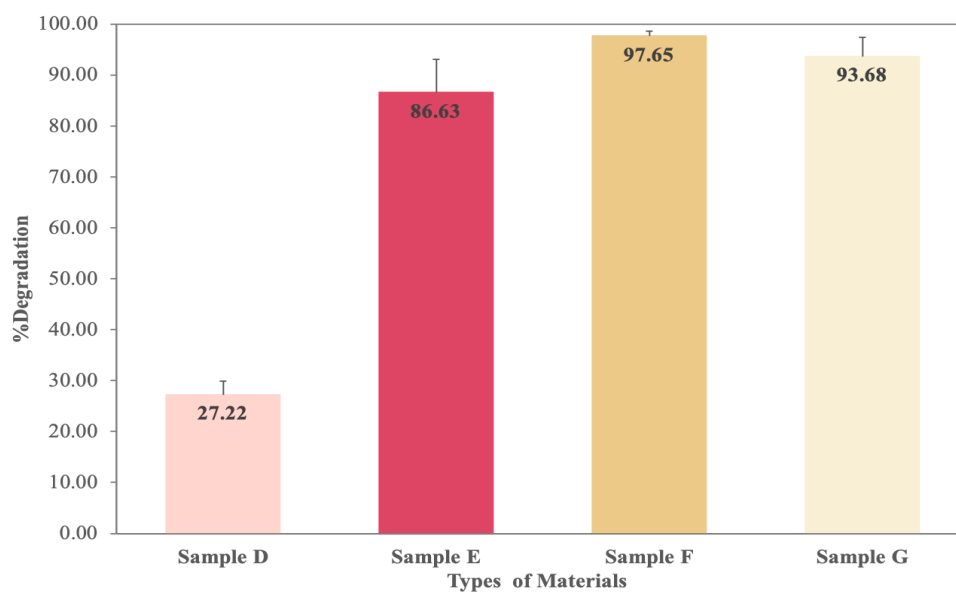

Figure 15. Comparison of photocatalytic degradation of four samples with different thickness of silica added: 1250TS37.5F_EtOH (Sample D), 1250TS150F_EtOH (Sample E), 1250TS600F_EtOH (Sample F), 1250TS900F_EtOH (Sample G)
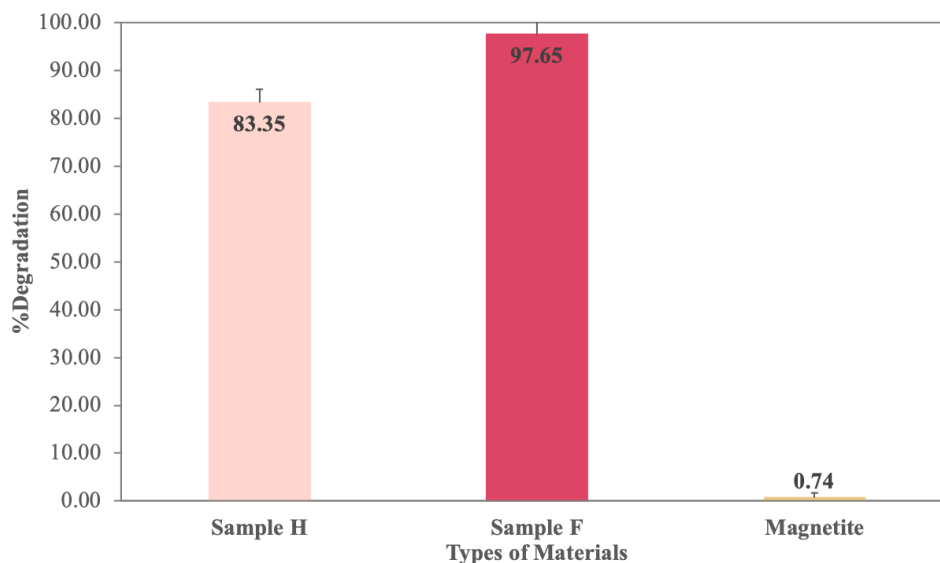
Figure 16. Comparison of photocatalytic degradation of three samples with different materials composing in nanocomposites: 1250Titania_EtOH (Sample H), 1250TS600F_EtOH (Sample F), Magnetite

3.3 Bactericidal activity

In this experiment, Titania-Silica-Iron oxide nanocomposites of 600 µL TEOS were used as a sample to study the bactericidal activity. According to Figure 17, the subculture of bacterial cells were treated with three different concentrations of the nanocomposites with conditional exposure to UV light and non-UV. The three different concentrations of nanocomposites included 0, 32, and 50 mg per 25 mL subculture, respectively. The control group was not treated with nanocomposites instead it was subdivided into two subgroups, which were the ones with UV light exposure and without UV light exposure. The number of survival cells were plotted on the bar chart as shown in the following Figure 19 after *E.coli* were treated with the nanocomposites under UV irradiation. In comparison, for the one using 32 mg/ 25 mL, there were 6.09 x 10^{-8} CFU/ mL recorded from the UV-exposed condition, while the one without UV irradiation was around 4.69 x 10^{-8} CFU/ mL. Moreover, there were 5.39 x 10^{-8} CFU/ mL of the survival bacteria cells observed after treating with 50 mg/ 25mL of nanocomposites. Therefore, the results indicated that Titania-Silica-Iron oxide nanocomposites of 600 µL TEOS were not effective in bactericidal activity towards *E.Coli,* and hence there were no significant bactericidal effects from the nanocomposites.

In contrast, P Chanhom et al. **[1,11]** had been reported that Titania-Silica-Iron oxide was really able to exhibit bactericidal activity toward *E. coli.* Upon the subculture of bacterial cells

treated with various concentrations of nanocomposites under UV light activated, it expressed that 99% of survival cells were dramatically reduced when the concentration of nanocomposites was kept adding until reaching 20.0 mg/L. Actually, the survival cells were gradually decreased by just initially adding 17.5mg/L of nanocomposites (Figure 18). Although, these nanocomposites compared to post-report [1] were constructed with the similar structural compositions of titania shell, silica interlayer and iron oxide core, but the efficiency in bactericidal activities were seemingly diverse. According to the previous research, bactericidal activity from titania could produce some superoxide anion and hydroxyl radical under activation of ultraviolet light which were originated from extreme toxic reactive oxygen species (ROS), as producing of ROS was significantly produced oxidative of bacterial cells membrane causing leakage and destruction of bacterial intracellular components such as cellular respiration and cellular metabolism, then the cell were died [6]. Thus, if the size of particles were too large to enter into the bacterial intracellular, this might make ROS just react outside of the cell membrane, which would be more difficult for ROS to integrate the chemical mechanism inside of the bacterial cell. This could be determined that the synthesized nanocomposites could not kill bacteria since their particle size is too large to enter into a bacteria cell [41]. According to the TEM image, our nanocomposite size is around 159.90 ± 29.578 nm which is quite large when compared to the previous work [11] as their nanocomposite size is around 108.5 ± 28.86 nm, this reason could be an argument why Titania-silica-iron oxide nanocomposites in this experiment were not as efficient as in P. Chanhom *et al.* paper [1,11].

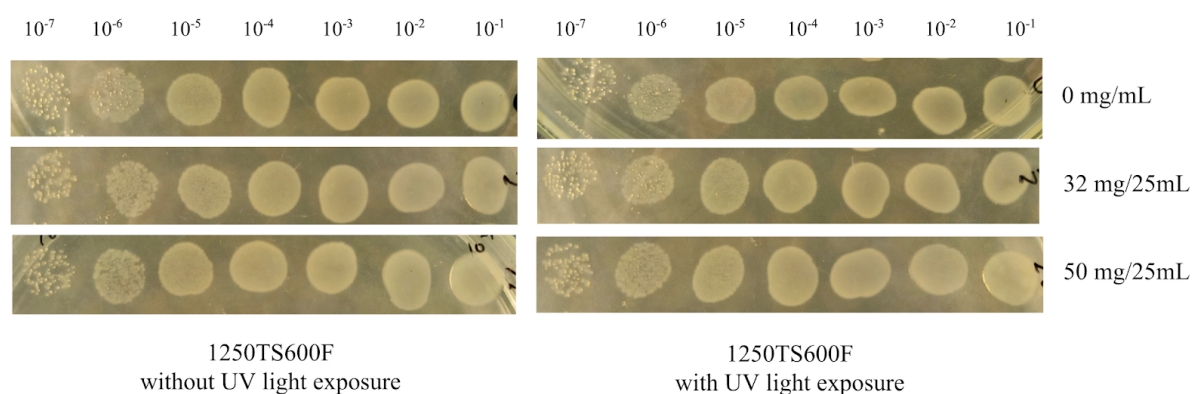**Figure 17.** The bactericidal activity of various concentration of 1250TS600F toward *E. coli* for both without (left) and with (right) UV light exposure
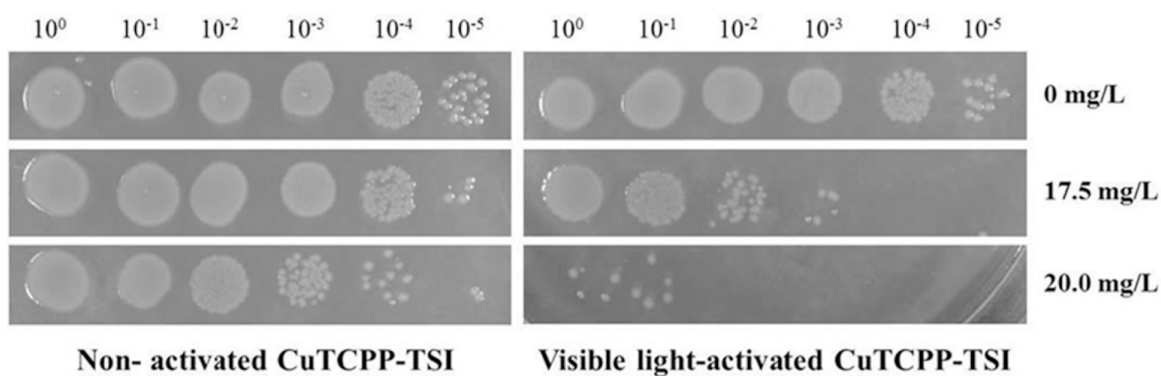
Figure 18. The bactericidal activity of CuTCPP-TSI (copper(II)tetra(4- carboxyphenyl)porphyrin -sensitized titania-silica-iron oxide nanocomposites) against *E. Coli* [1]
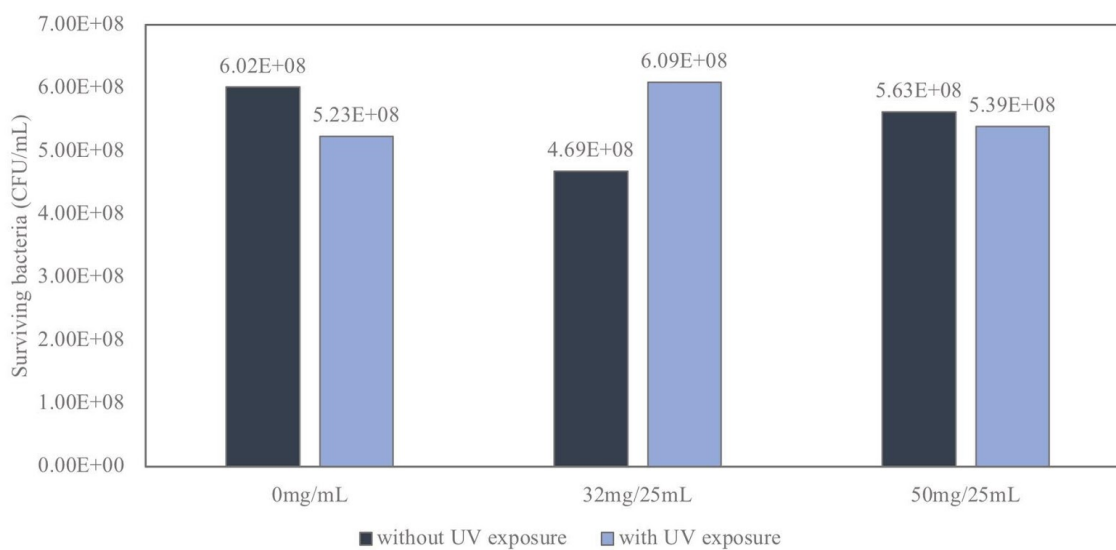

Figure 19. The bar chart shows number of surviving bacteria in CFU/mL from different conditions

Chapter 4
Conclusion

Titania-Silica-Iron oxide nanocomposites were completely synthesized with different amounts of silica added (37.5, 150, 300, 600 and 900 μL TEOS). The nanocomposites were also investigated the efficiency of photocatalytic activity by degradation of methylene blue under irradiation of UV light, the result show that the Titania-Silica-Iron oxide nanocomposites with 600μL TEOS can be the most effective in the degradation of Methylene Blue dye with the highest percentage of 97.65 as using 600 μL of TEOS for the synthesis of silica interlayer is the most suitable thickness to prevent the titania and magnetite from the electron and hole recombination. However, when comparing the diameter of the as-prepared synthesized nanocomposites from the SEM and TEM images to the nanocomposites from the previous works **[1, 11]**, the sizes of the nanocomposites from this experiment were bigger due to the difference in synthesis method. Therefore, the nanocomposites were not able to kill the bacteria, *E.coli.* Besides, the SEM result showed that all three components were successfully synthesized as titania, silica, and iron oxide was recovered on the material. Also, the technique for synthesis of the nanocomposites were prosperously able to produce in large gram - scale by comparing to P Chanhom et al. which was shown the product at 0.1005 g/batch, while in this experiment was shown at 0.4816 g/batch. Thus, this Titania-Silica-Iron oxide nanocomposite could also be proved to apply in wastewater treatment systems with removable and reusable magnets. On the other hand, the bactericidal activity in this case was not efficient to use for killing bacteria as compared to previous reports **[1, 11].**

References

[1] Chanhom, P., Charoenlap, N., Manipuntee, C., & Insin, N. (2019). Metalloporphyrins-sensitized titania-silica-iron oxide nanocomposites with high photocatalytic and bactericidal activities under visible light irradiation. *Journal of Magnetism and Magnetic Materials,475*, 602-610. doi:10.1016/j.jmmm.2018.11.090

[2] Dodoo-Arhin, D., Bowen-Dodoo, E., Agyei-Tuffour, B., Nyankson, E., Obayemi, J. D., Salifu, A. A., . . . Soboyejo, W. O. (2020). Modified nanostructured titania photocatalysts for aquatic disinfection applications. *Materials Today: Proceedings*. doi:10.1016/j.matpr.2020.07.710

[3] World Health Organization. (2018). E. coli. Retrieved November 17, 2020, from https://www.who.int/news-room/fact-sheets/detail/e-coli

[4] Pires, S. M., Majowicz, S., Gill, A., & Devleesschauwer, B. (2019). Global and regional source attribution of Shiga toxin-producing Escherichia coli infections using analysis of outbreak surveillance data. *Epidemiology and Infection,147*. doi:10.1017/s095026881900116x

[5] World Health Organization. (2020, November 17). Outbreaks of E. coli O104:H4 infection. Retrieved November 17, 2020, from https://www.euro.who.int/en/health-topics/disease-prevention/food-safety/outbreaks-of-e.-coli-o104 h4-infection

[6] Quisenberry, L. R., Loetscher, L. H., & Boyd, J. E. (2009). Catalytic inactivation of bacteria using Pd-modified titania. *Catalysis Communications,10*(10), 1417-1422. doi:10.1016/j.catcom.2009.03.013

[7] Kumar, S. P., Pavithra, G. K., & Naushad, M. (2019). Characterization techniques for nanomaterials. *Nanomaterials for Solar Cell Applications,*97-124. doi:10.1016/B978-0-12-813337-8.00004-7

[8] Ammar, S. H., Abdulnabi, W. A., & Kader, H. D. (2020). Synthesis, characterization and environmental remediation applications of polyoxometalates-based magnetic zinc oxide nanocomposites (Fe3O4@ZnO/PMOs). Environmental Nanotechnology, Monitoring & Management, 13, 100289. doi:10.1016/j.enmm.2020.100289

[9] Bao, X., Qiang, Z., Chang, J., Ben, W., & Qu, J. (2014). Synthesis of carbon-coated magnetic nanocomposite (Fe3O4@C) and its application for sulfonamide antibiotics removal from water. Journal of Environmental Sciences, 26(5), 962-969. doi:10.1016/s1001-0742(13)60485-4

[10] Kanakaraju, D., & Wong, S. P. (2018). Photocatalytic Efficiency of TiO2-Biomass Loaded Mixture for Wastewater Treatment. Journal of Chemistry, 2018, 1-14. doi:10.1155/2018/4314969

[11] Chanhom, P., Charoenlap, N., Tomapatanaget, B., & Insin, N. (2017). Colloidal titania-silica-iron oxide nanocomposites and the effect from silica thickness on the photocatalytic and bactericidal activities. *Journal of Magnetism and Magnetic Materials,427*, 54-59. doi:10.1016/j.jmmm.2016.10.123

[12] Guo, T., Lin, M., Huang, J., Zhou, C., Tian, W., Yu, H., . . . Feng, X. (2018). The Recent Advances of Magnetic Nanoparticles in Medicine. *Journal of Nanomaterials,2018*, 1-8. doi:10.1155/2018/7805147

[13] Creative Diagnostics. (n.d.). Properties and Applications of Magnetic Nanoparticles. Retrieved November 17, 2020, from
https://www.cd-bioparticles.com/t/Properties-and-Applications-of-Magnetic-Nanoparticles_55.html

[14] Sangaiya, P., & Jayaprakash, R. (2018). A Review on Iron Oxide Nanoparticles and Their Biomedical Applications. *Journal of Superconductivity and Novel Magnetism,31*(11), 3397-3413. doi:10.1007/s10948-018-4841-2

[15] Bu, A. (n.d.). Iron Oxide Nanoparticles, Characteristics and Applications. Retrieved November 17, 2020, from
https://www.sigmaaldrich.com/technical-documents/articles/technology-spotlights/iron-oxide-nano particles-characteristics-and-applications.html

[16] Arias, L., Pessan, J., Vieira, A., Lima, T., Delbem, A., & Monteiro, D. (2018). Iron Oxide Nanoparticles for Biomedical Applications: A Perspective on Synthesis, Drugs, Antimicrobial Activity, and Toxicity. *Antibiotics,7*(2), 46. doi:10.3390/antibiotics7020046

[17] Hernández-Hernández, A. A., Aguirre-Álvarez, G., Cariño-Cortés, R., Mendoza-Huizar, L. H., & Jiménez-Alvarado, R. (2020). Iron oxide nanoparticles: Synthesis, functionalization, and applications in diagnosis and treatment of cancer. *Chemical Papers,74*(11), 3809-3824. doi:10.1007/s11696-020-01229-8

[18] Speight, J. G. (2017). Industrial Inorganic Chemistry. *Environmental Inorganic Chemistry for Engineers,*111-169. doi:10.1016/b978-0-12-849891-0.00003-5

[19] Wu, Y. (2007). Preparation Of Ultrafine Powders By Reaction–Precipitation In Impinging Streams III: Nano Titania. *Impinging Streams,*301-315. doi:10.1016/b978-044453037-0/50045-8

[20] Ibrahim, H. M. (2015). Photocatalytic degradation of methylene blue and inactivation of pathogenic bacteria using silver nanoparticles modified titanium dioxide thin films. *World Journal of Microbiology and Biotechnology, 31*(7), 1049-1060. doi:10.1007/s11274-015-1855-9

[21] Pezzoni, M., Catalano, P. N., Delgado, D. C., Pizarro, R. A., Bellino, M. G., & Costa, C. S. (2020). Antibiofilm effect of mesoporous titania coatings on Pseudomonas aeruginosa biofilms. *Journal of Photochemistry and Photobiology B: Biology,203*, 111762. doi:10.1016/j.jphotobiol.2019.111762

[22] PubChem. (n.d.). Silicon dioxide. Retrieved November 17, 2020, from
https://pubchem.ncbi.nlm.nih.gov/compound/Silicon-dioxide

[23] Yu, X., Liu, S., & Yu, J. (2011). Superparamagnetic γ-Fe2O3@SiO2@TiO2 composite microspheres with superior photocatalytic properties. *Applied Catalysis B: Environmental,104*(1-2), 12-20. doi:10.1016/j.apcatb.2011.03.008

[24] Beydoun, D., Amal, R., Low, G., & Mcevoy, S. (2002). Occurrence and prevention of photodissolution at the phase junction of magnetite and titanium dioxide. *Journal of Molecular Catalysis A: Chemical,180*(1-2), 193-200. doi:10.1016/s1381-1169(01)00429-0

[25] Nishikiori, H., Matsunaga, S., Iwasaki, M., Zettsu, N., Yamakawa, M., Kikuchi, A., . . . Teshima, K. (2019). Formation of silica nanolayer on titania surface by photocatalytic reaction. *Applied Catalysis B: Environmental,241*, 299-304. doi:10.1016/j.apcatb.2018.09.046

[26] Samanta, I., & Bandyopadhyay, S. (2020). Escherichia coli. *Antimicrobial Resistance in Agriculture,*171-193. doi:10.1016/b978-0-12-815770-1.00015-8

[27] Marler Clark. (2020, November 17). Sources of E. coli. Retrieved November 17, 2020, from https://about-ecoli.com/ecoli_sources

[28] Felson, S. (2018, December 15). E. Coli Bacteria Infection: Symptoms, Treatment, Causes & Prevention. Retrieved November 17, 2020, from https://www.webmd.com/food-recipes/food-poisoning/what-is-e-coli

[29] Pradeep, T. (2008). CORE-SHELL NANOPARTICLES. In *Nano: The essentials: Understanding nanoscience and nanotechnology*. New York: McGraw-Hill.

[30] Bunaciu, A. A., Udriştioiu, E. G., & Aboul-Enein, H. Y. (2015). X-Ray Diffraction: Instrumentation and Applications. *Critical Reviews in Analytical Chemistry,45*(4), 289-299. doi:10.1080/10408347.2014.949616

[31] Asmatulu, R., & Khan, W. S. (2019). Characterization of electrospun nanofibers. *Synthesis and Applications of Electrospun Nanofibers,* 257-281. doi:10.1016/b978-0-12-813914-1.00013-4

[32] Shojaei, T. R., & Azhari, S. (2018). Fabrication, functionalization, and dispersion of carbon nanotubes. *Emerging Applications of Nanoparticles and Architecture Nanostructures,*501-531. doi:10.1016/b978-0-323-51254-1.00016-6

[33] Worsfold, P. (2005). SPECTROPHOTOMETRY | Overview. *Encyclopedia of Analytical Science,*318-321. doi:10.1016/b0-12-369397-7/00714-7

[34] Majidi, S., Sehrig, F. Z., Farkhani, S. M., Goloujeh, M. S., & Akbarzadeh, A. (2014). Current methods for synthesis of magnetic nanoparticles. Artificial Cells, Nanomedicine, and Biotechnology, 44(2), 722-734. doi:10.3109/21691401.2014.982802

[35] Liu, R., Wu, H. S., Yeh, R., Lee, C. Y., & Hung, Y. (2012). Synthesis and Bactericidal Ability of TiO2and Ag-TiO2Prepared by Coprecipitation Method. International Journal of Photoenergy, 2012, 1-7. doi:10.1155/2012/640487

[36] Dong, Y., Fei, X., Zhang, H., & Yu, L. (2015). Effects of Calcination Process on Photocatalytic Activity of TiO2/MCM- 41 Photocatalyst. *Journal of Advanced Oxidation Technologies,18*(2). doi:10.1515/jaots-2015-0219

[37] Lv, K., Xiang, Q., & Yu, J. (2011). Effect of calcination temperature on morphology and photocatalytic activity of anatase TiO2 nanosheets with exposed {001} facets. *Applied Catalysis B: Environmental,104*(3-4), 275-281. doi:10.1016/j.apcatb.2011.03.019

[38] Chen, Y., Lee, C., Yeng, M., & Chiu, H. (2003). The effect of calcination temperature on the crystallinity of TiO2 nanopowders. Journal of Crystal Growth, 247(3-4), 363-370. doi:10.1016/s0022-0248(02)01938-3

[39] Liu, S., Yu, B., Wang, S., Shen, Y., & Cong, H. (2020). Preparation, surface functionalization and application of Fe3O4 magnetic nanoparticles. *Advances in Colloid and Interface Science,281*, 102165. doi:10.1016/j.cis.2020.102165

[40] Giesriegl, A., Blaschke, J., Naghdi, S., & Eder, D. (2019). Rate-Limiting Steps of Dye Degradation over Titania-Silica Core-Shell Photocatalysts. Catalysts, 9(7), 583. doi:10.3390/catal9070583

[41] Díez-Pascual, A. M. (2020). Antibacterial Action of Nanoparticle Loaded Nanocomposites Based on Graphene and Its Derivatives: A Mini-Review. *International Journal of Molecular Sciences,21*(10), 3563. doi:10.3390/ijms21103563

Biography

Penpatcha Limsowan

Introductory, Miss Penpatcha Limsowan was born on July 28th, 1998 in Bangkok, Thailand. She completed school until her 12th grade from Saint Joseph Convent School in 2016. In 2017, she started her undergraduate degree in the Bachelor of Science in Applied Chemistry majoring in Material Chemistry at the Faculty of Science, Chulalongkorn University. Her current address is 316-136/1 Sainamthip Lane, Sukhumvit 22 Road, Khlong Toey Subdistrict, Khlong Toey District, Bangkok, Thailand, 10110.

As in the future plan, after graduating from the university, she will be studying for the master's degree of commerce and accountancy majoring in business administration in the international program.

Contact detail: penpatcha.lin@gmail.com

Chutima Rakyu

On the surface, Miss Chutima Rakyu was born on November 2nd, 1999 in Bangkok, Thailand. Her high school during grade 10 to grade 11 was initially graduated from Mahidol University International Demonstration School in 2016. Then, in the same year she continued to completely qualify for her high school diploma by taking the GED examination. After that, she started university life for her undergraduate degree in Bachelor of Science in Applied Chemistry (BSAC) in the major of Industrial Chemistry and Management, Faculty of Science, Chulalongkorn University. Currently, she is going to graduate her fourth year in 2020. Her current address is 67 Village no. 6, Bang Nam Chuet Subdistrict, Muang District, Samutsakhon,74000 Thailand.

In the near future, she has planned to proceed on her master's degree in the subject based on faculty of commerce and Accountancy in international programs including international business management, finance or business administration. However, every decision is still in progress before graduating from BSAC.

Contact detail: rakyu.nae@gmail.com